STUDY ON FLOW BOILING HEAT TRANSFER IN HORIZONTAL-RECTANGULAR-NARROW-FLAT CHANNELS

Y. Koizumi and K. Ohira*
Thermal and Fluid Engineering Group, Japan Atomic Energy Agency
Tokai-mura, Ibaraki, 319-1195, Japan
koizumiy@shinshu-u.ac.jp

ABSTRACT

This study is intended to examine to how large conventional results on the pressure drop and the heat transfer can be applicable when the channel size is decreased. By using deionized water, single-phase flow and flow boiling heat transfer experiments were performed for a thin rectangular channel of the width W = 3 mm and the height δ = 1.25 mm ~ 0.163 mm. The previous results of authors for the thin rectangular channel of the width W = 10 mm and the height δ = 1.1 mm ~ 0.18 mm were also utilized in analyzing results. The channel narrowness effect on the water single-phase flow heat transfer appeared when the hydraulic diameter D_{hy} became smaller than 1.06 mm. D_{hy} = 1.06 mm corresponds to δ = 0.640 mm for the present 3 mm width case and δ = 0.557 mm for the 10 mm width case. When the channel height became narrower than that size, the Nusselt number of the water single-phase flow heat transfer became smaller than that for a conventional size channel in the turbulent flow region. It also became dependent on the Reynolds number even in the laminar flow region. The modification method to incorporate the channel narrowness effect into the heat transfer coefficient correlation for the turbulent flow was proposed. The narrowness effect on the water single-phase flow pressure drop came out at D_{hy} = 0.714 mm i.e. δ = 0.405 mm for W = 3 mm and δ = 0.369 mm for W = 10 mm. When the channel height became narrower than that size, the friction factor in the laminar flow region became smaller than the value of a conventional size channel and transition from the laminar flow to the turbulent flow was delayed. The method to modify the friction factor equation of the laminar flow so as to be applicable to the narrow channel was proposed. In the flow boiling, when boiling started, churn flow appeared even at a low heat flux and a flow pattern was mainly the churn flow or/and the annular flow. The heat transfer coefficient was larger than that of pool boiling. The critical heat flux was higher than the value of Kutateladze correlation for the pool boiling. However, when the flow channel height became extremely narrow in the present experimental range, it became lower than the Kutateladze value. The evaporation heat transfer of a film on the heat transfer surface was dominant. When the modification for the single-phase flow heat transfer was introduced, the Dengler and Addoms correlation for the forced convection evaporation heat transfer for a conventional size channel predicted well present results.

KEYWORDS
Narrow Height Channel, Pressure Drop, Heat Transfer, Two-Phase Flow, Flow Boiling

1. INTRODUCTION

Flow and heat transfer are quite fundamental phenomena in usual size machines. Thus, numerous researches have been performed for these. When cooling an integrated circuit or leak flow from a pin hole

* Japan Steel Works Ltd., Funakoshi Minami, Aki-ku, Hiroshima-shi, Hiroshima, 736-0082, Japan

of a nuclear reactor and so on are considered, knowledge on thermal hydraulics for a small scale channel is required. This study is intended to examine pressure drop and heat transfer of the small scale channels.

If the flow area is scaled down, that effect is usually classified by the Knudsen number Kn of the ratio of the mean free path of molecules to the characteristic length of the flow path [1]. The boundary between the continuum flow and the slip flow is roughly 100 μm for gas and 1 μm for liquid.

When the flow path size is decreased from the conventional size to the boundary to slip flow, it has been proved that the friction factor has the same trend as that for the usual size although it is a little bit lower than the value of the conventional size flow path. The Nusselt number in the laminar flow region becomes to show dependency on the Reynolds number on the contrary to the conventional size flow path [2] ~ [6].

In the case of two-phase flow, the situation becomes more complicated. The interaction between gas and liquid is important in the two-phase flow. The interaction is closely related to interface shape. The interface shape becomes dependent on the flow path size as it becomes small. A surface tension effect may also relatively increase. Thus, as the flow path size is decreased down, the effect of the down-sizing of the flow path size may become prominent.

Serizawa et al. [7] have reported from their experiments for 20 ~ 100 μm tubes that although they observed a new flow pattern of ring flow, flow patterns were similar to those for the usual size flow path and were roughly correlated by the Mandhane flow pattern map [8] for conventional size pipes. Triplett et al. [9] conducted experiments for 1.09 ~ 1.49 mm tubes. They reported the difference of the flow patterns between the mini flow channels and the usual size flow path. Chung et al. [10] also observed the difference of the flow patterns, however, the flow patterns that they observed were a little bit different from what Triplett et al. have reported.

As for the pressure drop, Chung et al. stated that the separated model of Lockhart-Martinelli [11] correlated well with their data. Mishima and Hibiki [12] also pointed out that their data for tubes of 1 ~ 4 mm diameter were well correlated by the Chisholm and Laird correlation [13] with some modification. Pehlvian et al. [14] have reported from their experiments for tubes with the diameter of 0.8, 1.0 and 3.0 mm that the major sources of the discrepancies between experimental results and existing flow pattern maps were the difficulty of the definition of the flow patterns and the complex nature of the gas-liquid interface. They also pointed out about the pressure drop that the homogeneous model lost the accuracy as the flow channel size reached the micro size and the Chisholm model underpredicted the pressure drop. As stated above, it seems that even though the flow pattern and the pressure drop are the most fundamental items of the two-phase flow, clear results for these have not been obtained so far.

Kandlikar [15] has classified the flow channel by using the hydraulic diameter D_{hy} such as conventional channels (D_{hy} > 3 mm), minichannels (3 m ≥ D_{hy} > 200 μm), microchannels (200 μm ≥ D_{hy} > 10 μm, transition microchannels (10 μm ≥ D_{hy} > 1 μm), transition nanochannels (1 μm ≥ D_{hy} > 0.1 μm) and molecular nanochannels (0.1 μm ≥ D_{hy}). He has pointed out that nucleate boiling seems to be dominant in flow boiling in the microchannels. He concluded that further experimental research was necessary to develop more accurate models and predictive techniques for a flow boiling heat transfer coefficient and a critical heat flux (CHF) in the microchannles. Liu and Garimella [16] reported that the modified Chen model [17] provided good prediction for their flow boiling experimental results for parallel microchannels of 0.275 mm × 0.636 mm rectangular cross-section

It is clear that reliable results for predicting the pressure drop, the heat transfer coefficient and the CHF of boiling flow in mini- and micro-channels are still needed. Koizumi et al. [18] ~ [20] examined the pressure drop, the heat transfer and the CHF for the rectangular flow channels of the width W = 10 mm and the channel height δ = 0.18 mm ~ 1.1 mm. Results obtained so far was;

1. In the water single-phase flow condition, the narrowness effect came out around δ = 0.37 mm. Below that value, the friction factor became lower than the value of the conventional size flow path in the laminar flow region. The transition from the laminar flow to the turbulent flow was also delayed. The Nusselt number showed dependency on the Reynolds number even in the laminar flow region and became lower than the value for the conventional size flow path over the whole Reynolds number range.

2. Bubbly flow, slug flow, semi annular flow and annular flow were observed. The flow pattern transition agreed well with the Baker flow pattern map for the conventional size flow path.
3. The Martinelli and Nelson [21] method for the pressure drop of boiling two-phase flow predicted experimental results well. In the low quality region, measured pressure drop was larger than the predicted value because of sub-cooled boiling.
4. When the channel height was higher than 0.37 mm, a flow state was the bubbly flow until the CHF condition and the flow boiling heat transfer was well expressed with the Rohsenow pool boiling correlation [22]. When the channel height was narrower than 0.37 mm, a film flow state came out at an early stage after boiling initiation. Tiny bubbles were noted in the film on the heat transfer surface at a high heat flux. The heat transfer coefficient became larger than that of the Rohsenow pool boiling correlation because of the effective heat transfer of the evaporation of the film.
5. At the critical heat flux condition, the heat transfer surface was covered by a liquid lump, a large bubble pushed away the liquid lump, a dry area was formed on the heat transfer surface and then a liquid lump came around to cover the heat transfer surface again. This process repeated rapidly
6. The critical heat flux was lower than the value of the conventional size flow channel. The Koizumi and Ueda [23] method predicted well the trend of the critical heat flux.

In the present study, the channel width was decreased from 10 mm to 3 mm and the similar experiments on the single-phase flow heat transfer and the flow boiling heat transfer were performed for the channel height δ = 0.163 mm ~1.25 mm.

2. EXPERIMENTAL APPARATUS AND PROCEDURES

2.1. Experimental Apparatus

The experimental apparatus used in the present study is schematically shown in Fig. 1. The apparatus was composed of a water storage main-tank, water circulation pumps, a sub-tank for preheating test fluid and a test section. Deionized water was used in experiments.

The water storage main-tank was an open tank with a cover to protect it from dust. The main-tank had electric heaters to control water temperature. The water circulation pumps were canned-type gear pumps. The sub-tank was an open tank and had electric heaters. Water in the sub-tank was heated with the electric heaters up to the boiling condition at atmospheric pressure. A pipe coil in which test fluid flowed was submerged in the hot water in the sub-tank. Test fluid could be pre-heated up close to saturation temperature at atmospheric pressure.

Water pumped out from the main-tank by the circulation pumps flowed into the pre-heating section through a rotameter. The pre-heated test fluid flowed into the test section. Test fluid flowing out from the test section outlet returned to the main-tank.

Details of the test sections are presented in Fig. 2. The top cover of the test section is made of a transparent poly-carbonate plate which is one of acrylic resin for high temperature use. The bottom plate was a glass epoxy plate of 10 mm thick. The bottom plate has a slit of 3 mm wide and 50 mm long. A copper heat transfer surface of 3 mm wide and 50 mm long was inserted into the slit so as for the top surface to be flush with the bottom plate surface. The test section surface was finished with a #1,500 emery paper before every experiment. The bottom part of the heat transfer surface was thickened to 6 mm. The height of this part was 30 mm and there were three holes at every 7 mm in vertical direction and four holes in flow direction at every 10 mm for fixing thermocouples. Thus, there were twelve holes in total for the thermocouples. The bottom part of this thermocouple fixing section was further thickened to 80 mm to attach three 500 W electric cartridge heaters to heat the heat transfer surface.

A thin stainless plate was put between the top poly-carbonate plate and the bottom glass epoxy plate. The stainless plate had a slit of 3 mm wide and 260 mm long. This slit became a test flow channel. The gap i.e. the channel height δ was varied by changing the thickness of the stainless plate. O rings and a thin silicone sheet of 0.1 mm thick were used for sealing. The top poly-carbonate plate and the bottom glass epoxy plate were tightly fastened with eight bolts and nuts. The flow channel height δ was measured with

a laser displacement meter after fastening the test section. The measurement was performed at 15 points in the flow direction and 3 points in the width direction at each flow direction point. The average value at the 45 points was used as the channel height δ. The test section was fully covered with thermal insulator. After the experiment, the test flow channel height δ was confirmed again with the same measuring method.

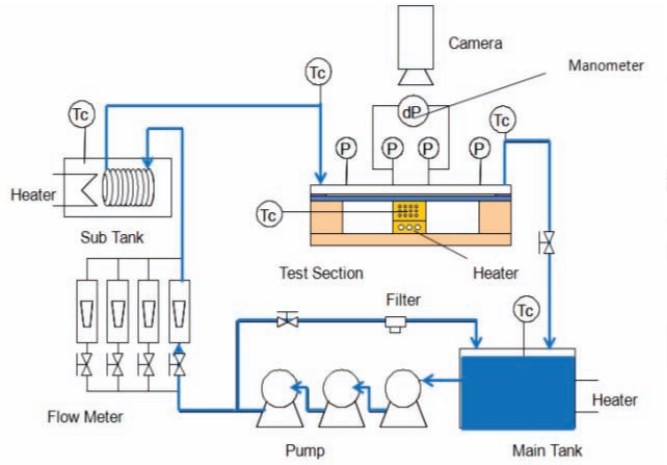

Fig. 1 Schematic Diagram of Experimental Apparatus

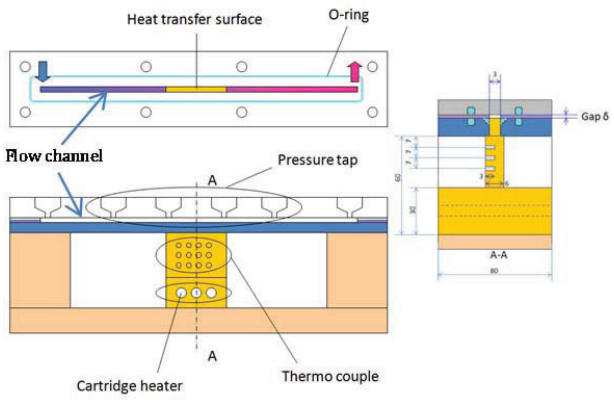

Fig. 2 Details of Test Section

The length and the width of the test flow channel were 260 mm and 3 mm, respectively. The heat transfer surface was at 115 mm from the inlet of the test flow channel. The length of the test heat transfer surface was 50 mm.

A flow rate was measured with rotameters. The flow rate was also measured by catching water flowing out from the outlet of the test section during certain time period. The rotameters were calibrated before experiments.

Fluid temperature was measured at the inlet and the outlet of the test section, and in the main-tank and the sub-tank with sheath chromel-alumel thermocouples. Heat transfer surface temperature was measured at twelve points also with sheath chromel-alumel thermocouples. The thermocouples were calibrated before experiments.

Surface temperature was derived by extrapolating the temperatures measured at three vertical locations. The surface heat flux was also derived from the temperatures measured at three vertical locations by using the Fourier law.

Pressure was measured at the inlet and the outlet of the test flow channel and also at the inlet and the outlet of the heat transfer section with Bourdon tubes. Pressure drop between the inlet and the outlet of the heat transfer section was measured with the manometer of Hg or Fluorinert FC-3283. The density of the Fluorinert FC-3283 is 1.83 kg/m^3. When the pressure drop was high, the Hg manometer was used. When the pressure drop was low, the Fluorinert manometer was used. When the Fluorinert manometer was used, a long time experiments was avoided to reduce the effect of the dissolution of the Fluorinert into water.

A flow state was recorded with a high speed video camera up to 2,000 frames/second.

The flow channel gap δ was ranged from 0.163 mm to 1.25 mm in the present study.

2.2. Experimental Procedure

A water storage main-tank was filled with distilled water. Then, using a bypass line between a pump and the tank, water was circulated. There was a filter of 5 μm mesh in the bypass line. The water in the tank was cleaned up by this bypass circulation. Then, the water was circulated in the test flow channel.

2.2.1. Single-phase pressure drop experiments

The temperature of test fluid was set at room temperature. A flow rate to the test section was fixed at a pre-determined value. Waiting for a while after it was confirmed that the movement of liquid surface in the manometer ceased, a flow rate and a pressure drop were measured. Then, the same procedure was iterated after the flow rate was increased by a prescribed value.

2.2.2. Single-phase heat transfer experiments

The temperature of test fluid at the test section inlet was set at room temperature. A flow rate to the test section and heat input to cartridge heaters of the test section were fixed at pre-determined values, respectively. Waiting for a while after it was confirmed that the movement of liquid surface in the manometer ceased and that heat transfer surface temperatures and the fluid temperature at the outlet of the test section were fully stabilized, a flow rate, a pressure drop, the heat transfer surface temperatures and the fluid temperatures at the inlet and the outlet of the test section were measured. Then, the same procedure was iterated after the flow rate was increased by a prescribed value.

2.2.3. Flow boiling heat transfer experiments

The test fluid temperature at the inlet of the test section was set at approximately 98 °C. A flow rate to the test section was fixed at a pre-determined value. Then, electric power supply for the heaters of the test section was increased stepwise. After it was confirmed that the flow condition and test section temperatures were fully stabilized at each step, the flow rate, pressure at the heating test section inlet, pressure drop between the inlet and the outlet of the heating test section, water temperatures at the inlet and the outlet of the test section and the temperatures of the heating test section at twelve locations were recorded. A flow state was recorded from top through the transparent top cover of the test section by a high speed video camera at 2,000 frames/s. This procedure was iterated until the surface temperature of the heating test section showed an unstable state such as it fluctuated or kept going up. The flow channel height δ tested in the present experiments was in a range from 0.163 mm to 1.25 mm. The hydraulic diameter D_{hy} was from 0.309 mm to 1.76 mm.

It was sometimes observed in preparatory experiments that bubbles generated in the test flow channel moved oscillatory back and forth. Large flow resistance was added between the pump outlet and the test flow channel to avoid it. After the large resistance was introduced, the bubbles never went back and a float in a rotameter did not show fluctuation. Thus, a constant-steady flow rate at the inlet of the test section was maintained in the flow boiling heat transfer experiments.

3. EXPERIMENTAL RESULTS AND DISCUSSIONS

3.1. Single-Phase Flow Heat Transfer

In experiments, a local heat transfer coefficient h was calculated as follows;

$$h = \frac{q_w}{T_w - T_l} \tag{1}$$

Here q_w and T_w are the surface heat flux and the surface temperature at each temperature measurement location of the heating test section, respectively. T_l is the water temperature there calculated by interpolating the water temperatures measured at the inlet and the outlet of the test section. Then, the average value of the heat transfer coefficients at four locations was calculated. The average heat transfer coefficient was set as the heat transfer coefficient for that test condition in the single-phase flow heat transfer experiments.

The results of the single-phase flow heat transfer experiments are presented in Figs. 3 ~ 6. In the figures, the Nusselt number

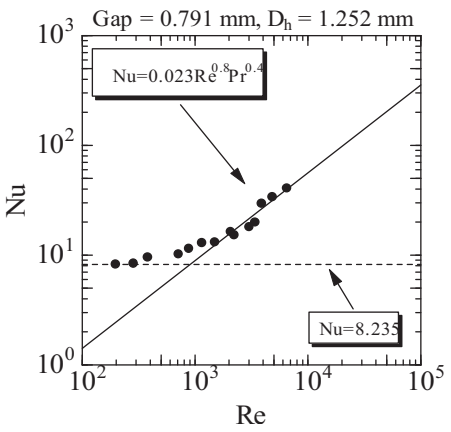

Fig. 3 Single-Phase Flow Heat Transfer Coefficient (δ = 0.791 mm)

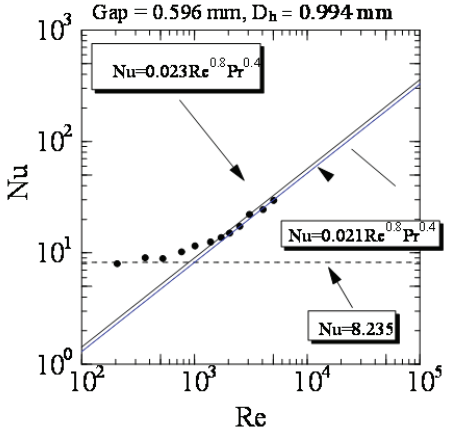

Fig. 4 Single-Phase Flow Heat Transfer Coefficient (δ= 0.596 mm)

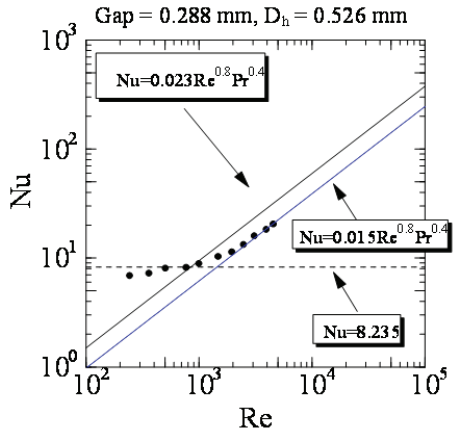

Fig. 5 Single-Phase Flow Heat Transfer Coefficient (δ= 0.288 mm)

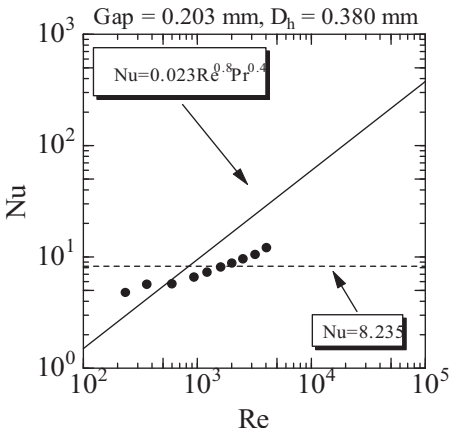

Fig. 6 Single-Phase Flow Heat Transfer Coefficient (δ= 0.203 mm)

$$Nu = \frac{hD_{hy}}{k_l} \tag{2}$$

is plotted against the Reynolds number. Here, Dhy is the hydraulic diameter and k_l is the thermal conductivity of water, respectovely. In the figure, the Nusselt number for laminar flow between infinite-parallel plates (Özişik [24])

$$Nu = 8.235 \tag{3}$$

and the Nusselt number of the Dittus-Boelter correlation for turbulent flow in a flow channel

$$Nu = C\,\mathrm{Re}^{0.8}\,\mathrm{Pr}^{0.4}, \quad C = 0.023 \tag{4}$$

are also shown for comparison with a dashed line and a solid line, respectively. In Eq. (4), Pr is the Prandtl number of water and Re is the Reynolds number

$$Re = \frac{u_l D_{hy}}{\nu_l} \tag{5}$$

Here, u_l is the water velocity and ν_l is the water kinematic viscosity, respectively.

It should be noted that Eq. (3) is for the condition that top and bottom walls are heated uniformly, but only the bottom wall was heated in the present experiments.

In Fig. 3 where δ = 0.791 mm, the measured results agree well with the values of Eq. (4) when Re > 2,000. As Re becomes smaller than 2,000, the measured results deviate from Eq. (4) and approach to the value of Eq. (3). It suggests that the flow transition from the turbulent flow to the laminar flow starts around Re ≈ 2,000 with a decrease in Re.

In Fig. 4 where δ = 0.596 mm, similar trend to Fig. 3 is observed although the measured results are a little bit smaller than the values in Fig. 3 and the values of Eq. (4) in the turbulent flow region.

As δ is farther decreased, some difference comes out as shown in Fig. 5 where δ = 0.288 mm. The Nusselt number is smaller than the value of Eq. (4) in the turbulent flow region and weak dependency of the Nusselt number on the Reynolds number in the laminar flow region. These differences becomes more prominent in Fig. 6 where δ = 0.208 mm.

The best fit coefficient C of the right hand side of Eq. (4) was found as presented in Figs. 4 and 5 with dotted lines. Results so derived are plotted against the hydraulic diameter D_{hy} in Fig. 7. In the figure, results of Koizumi et al. [18] ~ [20] for 10 mm width experiments are also included. Clear dependency of the coefficient C on D_{hy} that C decreases with a decrease in D_{hy} is noticed irrespective of the channel width. The dependency of C on D_{hy} is approximated with linear relation as

$$C = 0.018 D_h + 0.004 \ , \ D_{hy} < 1.06 \text{ mm} \tag{6}$$

The boundary that C starts to decrease is D_{hy} = 1.06 mm i.e. δ = 0.640 mm for the 3 mm width case and δ = 0.557 mm for the 10 mm width case. It implies that the effect of narrowness on the water single-phase flow heat transfer comes out below that size. It should be noted that Eq. (6) is dimensionally incomplete. Although the dimension of D_{hy} is mm, C itself is dimensionless. Farther examination is required.

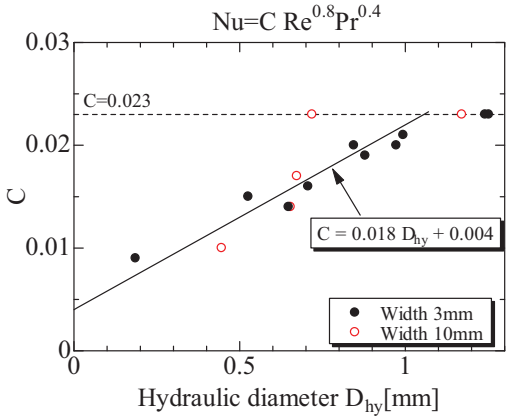

Fig. 7 Coefficient of Dittus-Boelter Correlation

3. 2. Single-Phase Flow Pressure Drop

Results of single-phase flow pressure drop experiments are illustrated in Figs. 8 ~ 11. The results are presented in the relation between the friction factor λ and the Reynolds number. In the figure, the friction factor for the laminar flow in a rectangular duct [25]

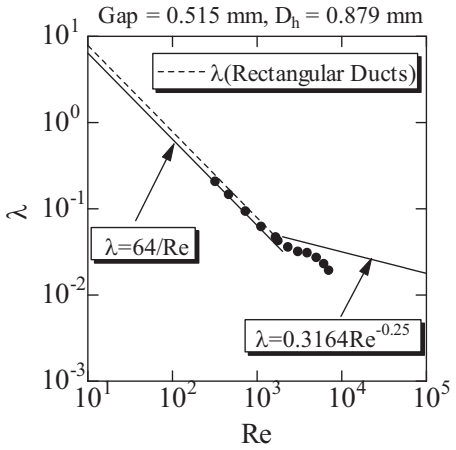

Fig. 8 Single-Phase Flow Friction Factor (δ = 0.515 mm)

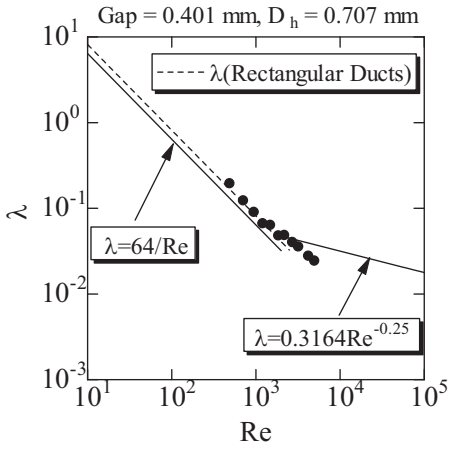

Fig. 9 Single-Phase Flow Friction Factor (δ = 0.401 mm)

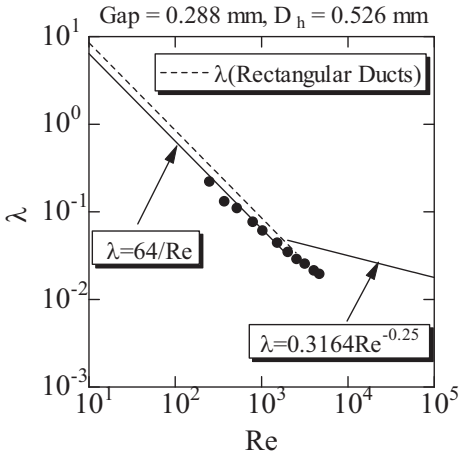

Fig. 10 Single-Phase Flow Friction Factor (δ = 0.288 mm)

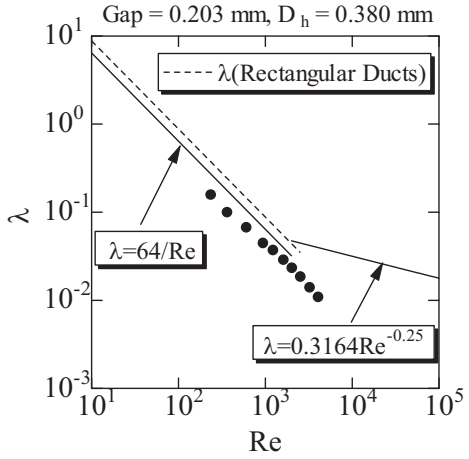

Fig. 11 Single-Phase Flow Friction Factor (δ = 0.203 mm)

$$\lambda = \frac{64}{\mathrm{Re}} \frac{3/2}{(1+\varepsilon)^2 \left\{ 1 - \frac{192}{\pi^5} \varepsilon (\tanh \frac{\pi}{2\varepsilon} + \frac{1}{3^5} \tanh \frac{\pi}{2\varepsilon} + ...) \right\}}, \tag{7}$$

the friction factor for laminar flow in a pipe

$$\lambda = \frac{64}{\mathrm{Re}} \tag{8}$$

and the Blasius friction factor for a turbulent flow in a pipe

$$\lambda = \frac{0.3164}{\mathrm{Re}^{0.25}} \tag{9}$$

are included for comparison. Here, ε is the ratio of the channel height δ and the channel width.

In Fig. 8 where the channel height δ = 0.515 mm, the measured friction factors agree well with the values of Eq. (7). The measured friction factor turns to deviate from the value of Eq. (7) around Re ≈ 1,000 and becomes to follow the trend of Eq. (9). It suggests that the flow turns to the laminar to the turbulent flow around there. The measured friction factors are a little smaller than the values of Eq. (7).

In Fig. 9 where δ = 0.401mm, the measured fiction factor agree well with the values of Eq. (7). However, the measured friction factors continue to decrease with an increase in Re even in the region supposed to be turbulent flow in the experimental range.

In Fig. 10 where δ = 0.288 mm, the measured friction factors are a little smaller than the values of Eq. (7) in the laminar flow region. The measured friction factors continue to decrease with an increase in Re even in the region supposed to be turbulent flow as in Fig. 9.

In Fig. 11 where δ = 0.203 mm, the measured friction factors are smaller than the values of Eq. (7) in the laminar flow region. The difference between the measured values and the values of Eq. (7) in Fig. 11 is larger than that in Fig. 10. The measured friction factors continue to decrease with an increase in Re even in the region supposed to be turbulent flow as in Figs. 9 and 10. Those results are the same as those for the channel width W = 10 mm [18] ~ [20].

For the laminar flow condition, how much the friction factor decreased from the value of Eq. (7) was derived from the present experimental results. The decreasing ratios C' from the value of Eq. (7) are plotted in Fig. 12. This result is approximated as

$$\frac{\lambda_{measured}}{\lambda_{Eq.(7)}} = C' = 1.4 D_{hy}, \quad D_{hy} < 0.714 \text{ mm} \tag{10}$$

It should be noted again that Eq. (10) is dimensionally incomplete. Although the dimension of D_{hy} is mm, C' itself is dimensionless. Farther examination is required.

D_{hy} = 0.714 mm corresponds to δ = 0.405 mm for the 3 mm width case and δ = 0.369 mm for the 10 mm width case. It implies that the effect of narrowness on the laminar water single-phase flow pressure drop comes out below that size.

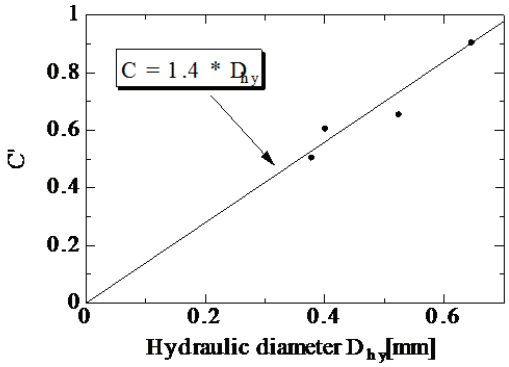

Fig. 12 Friction Factor Decreasing Ratio in Laminar Flow

3.3 Flow Boiling Heat Transfer Experiments

3.3.1 Flow pattern

Flow patterns observed in the present boiling heat transfer experiments are mainly slug flow and annular flow. When phase change i.e. boiling started in the test flow channel, the flow pattern turned from liquid single-phase flow to the churn flow directly. The typical example of the flow patterns observed in

the present experiments is shown in Fig. 13 comparing with the Baker flow pattern map [26]. Experimental points are distributed in the annular and the slug flow region.

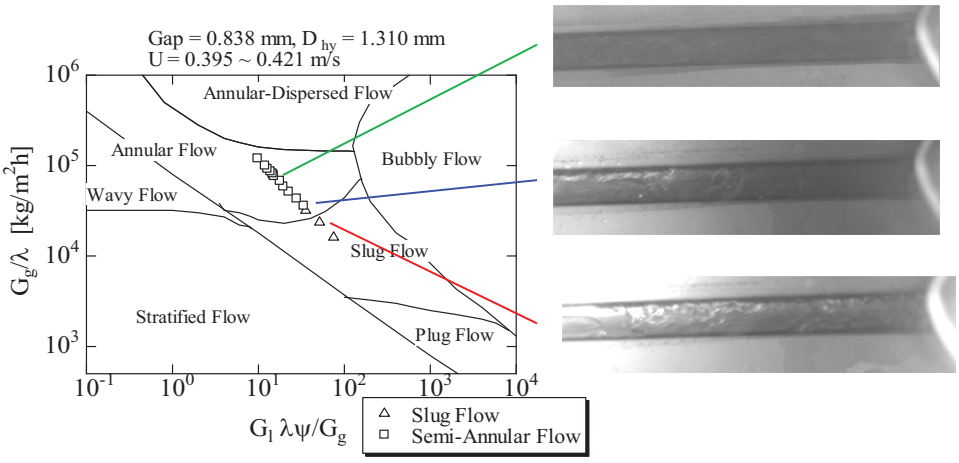

Fig. 13 Flow Pattern

3.3.2 Flow boiling heat transfer

Experimental results of flow boiling experiments are presented in the form of a boiling curve in Figs. 14 ~ 17. In the figures, the onset condition of nucleate boiling by the Bergles and Rohsenow correlation [27], the nucleate pool boiling relation by the Rohsenow correlation [22] and the critical heat flux of saturated pool boiling by the Kutateladze correlation [28] are illustrated with a dotted line and solid lines, respectively for comparison. Final plots in figures correspond to the critical heat flux (CHF) condition. The CHF condition was defined in the present experiments as the point that a further increase in the heat flux from that condition resulted in surface temperature fluctuation or the excursion of the heat transfer surface temperature.

In Figs. 14 ~ 17, the inclinations of plots in the boiling curve are milder than that of the Rohsenow correlation value. It should be noted that data plots are in the smaller wall super heat region than that of the Rohsenow correlation. It suggests that the flow boiling heat transfer coefficient was larger than the pool boiling. The critical heat fluxes for δ = 0.838 mm ~ 0.472 mm are larger than those of the Kutateladze correlation. The critical heat flux for δ = 0.273 mm is smaller than that of the Kutateladze correlation. Further examination is required for those results.

Heat transfer coefficients h_{TP} in the case of δ = 0.838 mm are presented in Fig. 18. In the figure, the measured heat transfer coefficient was divided by the single-phase water flow heat transfer coefficient h_{L0} of Eq. (4). In this calculation, the water velocity is decided by assuming that the total mas flow rate of vapor and liquid flows in the channel as water. The solid line in the figure exhibits the values of the Dengler and Addoms correlation [28]

$$\frac{h_{TP}}{h_{L0}} = 3.5\left(\frac{1}{X_{tt}}\right)^{0.5} \tag{11}$$

for the forced convection evaporation heat transfer. Here, X_{tt} is the Lockhart - Martinelli parameter [11] for turbulent - turbulent flow.

$$X_{tt} = \left(\frac{1-x}{x}\right)^{0.9}\left(\frac{\rho_g}{\rho_l}\right)^{0.5}\left(\frac{\mu_l}{\mu_g}\right)^{0.1} \tag{12}$$

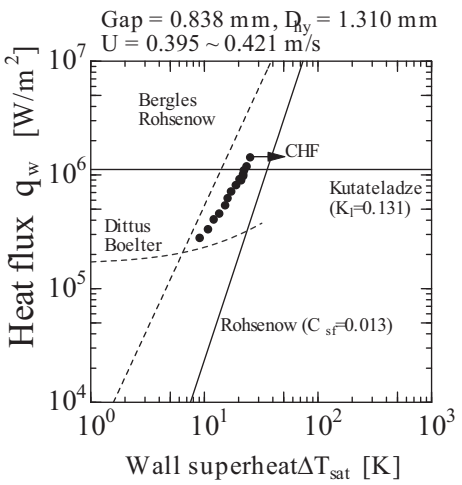

Fig. 14 Boiling Curve (δ = 0.838 mm)

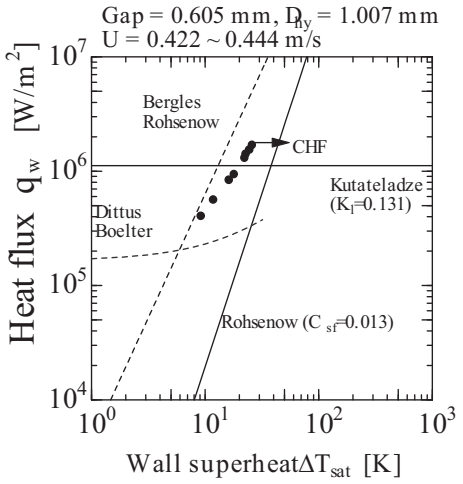

Fig. 15 Boiling Curve (δ = 0.605 mm)

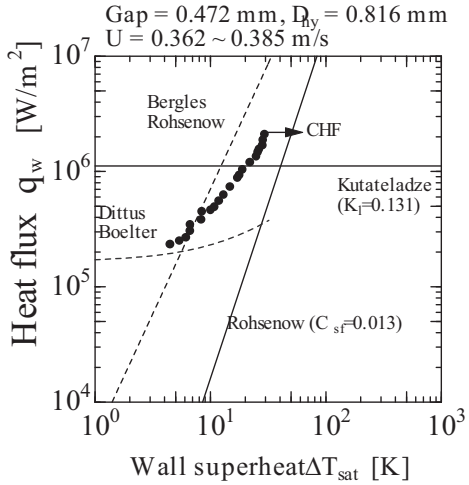

Fig. 16 Boiling Curve (δ = 0.472 mm)

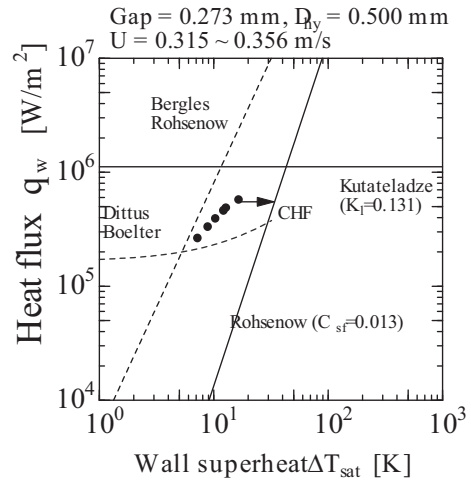

Fig. 17 Boiling Curve (δ = 0.273 mm)

Here, x is the vapor quality. Greek symbols ρ and μ are the density and viscosity, respectively. Subscripts g and l denote gas band liquid, respectively.

In Fig. 18, when the heat flux is low and the quality is low, boiling is dominant. Then, as the heat flux and the vapor quality increase, data plots come to follow the Dengler and Addoms relation. It implies that the evaporation of a film on the heat transfer surface becomes dominant and the heat transfer is augmented than boiling, which is well reflected in the boiling curve in Fig. 14.

Heat transfer coefficients in the case of δ = 0.163 mm are presented in Fig. 19. Solid symbols are measured results. The Dengler and Addoms correlation overpredicted the heat transfer coefficient. It was pointed out in section 3.1 that when the channel height got narrow, the single-phase heat transfer coefficient became smaller than the value of Eq. (4) in the turbulent flow region and it was proposed to modify Eq. (4) by using Eq. (6). When this modification is performed, data plots come close to the Dengler and Addoms relation as shown by open symbol in Fig. 19.

Other results of the two-phase flow heat transfer with the modification of Eq. (6) are presented in Fig. 20. It is concluded that the Dengler and Addoms correlation could be applicable to predict the two-phase flow heat transfer coefficient until 0.16 mm if the modification for the channel narrowing effect is introduced into the liquid single-phase flow heat transfer coefficient.

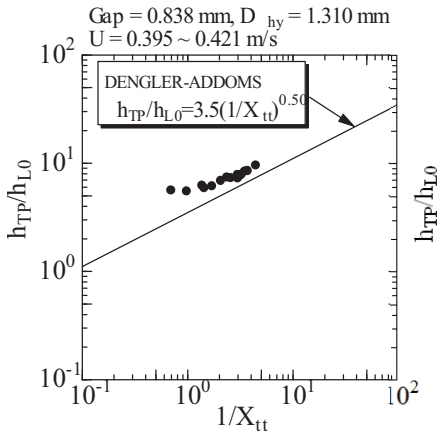

Fig. 18 Two-Phase Flow Boiling Heat Transfer (δ = 0.838 mm)

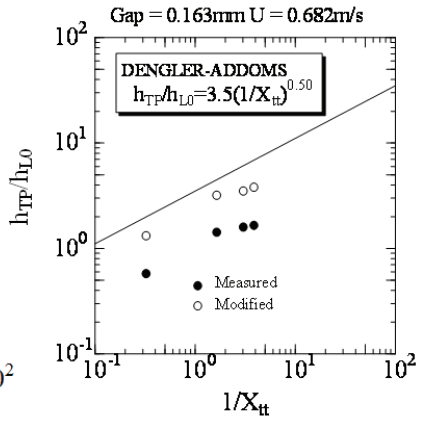

Fig. 19 Two-Phase Flow Boiling Heat Transfer (δ = 0.163 mm)

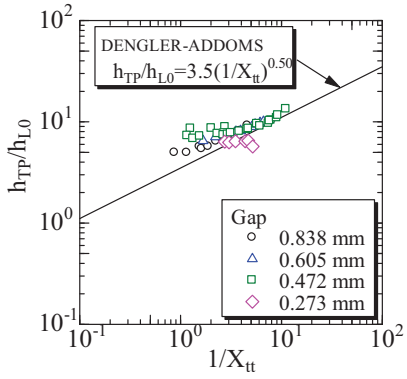

Fig. 20 Two-Phase Flow Boiling Heat Transfer

3.3.3 Two-phase flow pressure drop

Martinelli and Nelson [21] presented the method to predict the pressure drop during forced-circulation boiling of water. Present results are compared with that prediction. If the inlet condition of the flow channel is saturated, the ratio of the two-phase flow pressure drop ΔP_F in the boiling channel to the single-phase flow pressure drop ΔP_{L0} of saturated-water in the case that the flow rate is equal to the total mass flow rate is expressed as

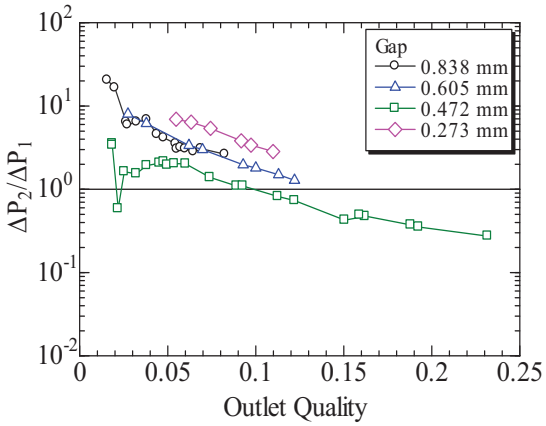

Fig. 21 Two-Phase Flow Pressure

$$\frac{\Delta P_F}{\Delta P_{Lo}} = \frac{1}{L}\int_0^L \left[\left(\frac{dP}{dz}\right)_F \Big/ \left(\frac{dP}{dz}\right)_{Lo}\right] = \frac{1}{x_e}\int_0^{x_e} (1-x)^{2-n}\,\Phi_{Ltt}{}^2\,dx \tag{13}$$

where L is the channel length, P is the pressure, x is the quality, x_e is the exit quality, z is the flow direction coordinate and Φ_{Ltt} is the two-phase flow pressure drop multiplier. The exponent n is 0.2 or 0.25 for turbulent flow. The inlet condition in the present experiments was sub-cooled. Thus, the saturation point was estimated from the heat flux and the flow rate, and then Eq. (13) was applied to the saturated

region. The pressure drop between the inlet of the flow channel and the saturation point could be derived from the single-phase flow pressure drop relation i.e. Eqs. (7) and (10).

The two-phase flow pressure drop ΔP_1 for the two-phase flow region calculated with Eq. (13) and the measured two-phase flow pressure drop ΔP_2 that is obtained by subtracting the single-phase region pressure drop calculated with Eqs. (7) and (10) from the pressure drop measured between the inlet and the outlet of the heating section are compared in Fig. 21. The Martinelli and Nelson method may predict the two-phase flow pressure drop for the present conditions. However, data are limited. It is hard to derive a conclusion at this stage. Farther examination is definitely required.

4. CONCLUSIONS

By using deionized water, single-phase flow and flow boiling heat transfer experiments were performed for a thin rectangular channel of the width W = 3 mm and the height δ = 1.25 mm ~ 0.163 mm. Following conclusions were obtained from the present experimental results and the previous experimental results of authors for the thin rectangular channel of the width W = 10 mm and the height δ = 1.1 mm ~ 0.18 mm.

1. The channel narrowness effect on the water single-phase flow heat transfer appeared when the hydraulic diameter D_{hy} became smaller than 1.06 mm. D_{hy} = 1.06 mm corresponds to δ = 0.640 mm for the present 3 mm width case and δ = 0.557 mm for the 10 mm width case. When the channel height became narrower than that size, the water single-phase flow heat transfer Nusselt number became smaller than that for a conventional size channel in the turbulent flow region. It also became dependent on the Reynolds number even in the laminar flow region. The modification method to incorporate the channel narrowness effect into the Dittus-Boelter correlation for the turbulent flow was proposed. That was to change the coefficient from 0 023 to 0.018 D_{hy} + 0.004 (dimensionless) for D_{hy} < 1.06 mm.
2. The narrowness effect on the water single-phase flow pressure drop came out around the hydraulic diameter D_{hy} = 0.714 mm i.e. δ = 0.405 mm for W = 3 mm and δ = 0.369 mm for W = 10 mm. When the channel height became narrower than that size, the friction factor in the laminar flow region became smaller than the value of a conventional size channel. Transition from the laminar flow to the turbulent flow was also delayed. The method to modify the friction factor equation of the laminar flow so as to be applicable to the narrow channel was proposed. That was to multiply the laminar friction factor by C' = 1.4D_{hy} (dimensionless) for D_{hy} < 0.714 mm.
3. In the flow boiling, when boiling started, churn flow appeared even at a low heat flux and a flow pattern was mainly the churn flow or/and annular flow. The heat transfer coefficient was larger than that of pool boiling. The critical heat flux was higher than the value of the Kutateladze correlation for the pool boiling. However, when the flow channel height became extremely narrow in the present experimental conditions, it became lower than the Kutateladze value.
4. In the flow boiling, the evaporation heat transfer of a film on the heat transfer surface was dominant. When the modification for the single-phase flow heat transfer was introduced, the Dengler and Addoms correlation for the forced convection evaporation heat transfer for a conventional size channel predicted well present results.

REFERENCES

1. Kandlihkar, S. G. and Grande, W. K., "Evaluation of Microchannel Flow Passages – Thermohydraulic Performance and Fabrication Technology", *Proc. ASME IMECE*, CD-ROM, IMECE2002-32043 (2002).
2. Wu, P. and Little, W. A., "Measurement of Friction Factors for the Flow of Gases in Very Fine Channels Used for Microminiature Joule-Thomson Refrigerators", *Cryogenics*, **Vol. 23**, pp273 (1983).
3. Wu, P. and Little, W. A., "Measurement of the Heat Transfer Characteristics of Gas Flow in Done Channel Heat Exchanger Used Microminiature Refrigerators", *Cryogenics*, **Vol. 24**, pp415 (1984).

4. Pfahler, J., Harley, J., Bau, M and Zemel, J. N., "Gas and Liquid Flow in Small Channel", Micromechanical Sensors, ASME DSC-**Vol. 32**, pp49 (1991).
5. Choi, S. B., Barron, R. F. and Warrinton, R. O., "Liquid Flow and Heat Transfer in Microtubes", ASME DSC-**Vol. 32**, pp123 (1991).
6. Wang, B. X. and Peng, X. F., "Experimental Investigation on Liquid Forced Convection Heat Transfer through Microchannels", *Int. J. Heat Mass Transfer*, **Vol. 37**, pp73 (1994).
7. Serizawa, A., FEN, Z. and Kawahara, Z., "Two-Phase Flow in Micro Channel", *Proc. JSMF Annual Meeting 2002*, pp29 – 31 (2002).
8. Mandhane, J. M., Gregory, G. A. and Azik, K., 1974. A flow pattern Map for Gas-Liquid Flow in Horizontal Pipes, Int. J. of Multiphase Flow, Vol. 1, No. 4, 537-553.
9. Triplett, K. A., Ghiaasiaan, S. M., Abdel-Khalik, S. I. and Sadowski, D. L., "Gas-liquid Two-Phase Flow in Microchannels, Part I: Two-Phase Flow Patterns", *Int. J. of Multiphase Flow*, **Vol. 25**, pp377-394 (1999).
10. Chung, P. M. Y., Kawaji, M., Kawahara, A. and Shibata, Y., "Two-Phase Flow through Square and Circular Microchannels –Effect of Channel Geometry", *Proc. the 6th ASME-JSME Thermal Engineering Joint Conference*, CD-ROM FED-AJ03 (2003).
11. Lockhart, R. W. and Maritinelli, R. C., "Proposed Correlation of Data for Isothermal Two-Phase Two-Component Flow in Pipes", *Chem Eng. Progress*, **Vol. 45**, pp39-48 (1949).
12. Mishima, K. and Hibiki, T., "Some Characteristics of Air-Water Two-Phase Flow in Small Diameter Vertical Tubes", *Int. J. Multiphase Flow*, **Vol. 22**, No. 4, pp703-712 (1996).
13. Chisholm, D. and Laird, A. D. K., "Two-Phase Flow in Rough Tubes", *Trans. ASME*, **Vol. 80**, No. 2, 276-286 (1958).
14. Pehlivan, K., Hassan, I. and Vaillancourt, M., "Experimental Study on Two-Phase Flow and Pressure Drop in Millimeter-size Channels", *Applied Thermal Engineering*, **Vol. 26**, pp1506-1514 (2006).
15. Kandlihkar, S. G., "Heat Transfer Mechanisim during Flow Boiling in Microchannels", *Trans. ASME J. of Heat Transfer*, **Vol. 126**, No. 1, pp8 - 16 (2004).
16. Liu, D. and Garimella, S. V., "Flow Boiling in Microchannel Heat Sink", *Proc. 2005 ASME IMECE*, CD-ROM IMECE2005-79555 (2005).
17. Chen, J. C., "A Correlation for Boiling Heat Transfer to Saturated Fluids in Convective Flow", ASME Paper 63-HT-34 (1963).
18. Koizumi, Y., Yamada, T. and Ohtake, H., "Flow Boiling Heat Transfer and Two-Phase Flow Pressure Drop in Thin-Rectangular Channels", *Proc. ASME ICNMM2008*, CD-ROM ICNMM2008-62026 (2008).
19. Koizumi, Y., Ohtake, H. and Yamada, T., "Flow Behavior and Flow Boiling Heat Transfer in Thin-Rectangular Mini-Channels", *Proc. ASME IMECE*, CD-ROM IMECE2008-66928 (2008).
20. Koizumi, Y., Ohtake, H. and Sato, K., "Pressure Drop and Heat Transfer of Single-Phase Flow and Two-Phase Flow in Thin-Rectangular Channels", *Proc. 7th International Conference on Multiphase Flow*, ICMF2010 CD-ROM 17.2.2 (2010).
21. Martinelli, R. C. and Nelson, D. B., "Prediction of Pressure Drop during Forced-Circulation Boiling of Water", *Trans. ASME*, **Vol. 70**, pp695-702 (1948).
22. Rohsenow, W. M., "A Method of Correlating Heat Transfer Data for Surface Boiling Liquid", *Trans. ASME*, **Vol. 74**, pp969-976 (1952).
23. Koizumi, Y., Matsuo, T., Miyota, Y. and Ueda, T., "Dry-out Heat Fluxes of Falling Film and Low-Mass Flux Upward Flow in Heated Tubes", *Trans. JSME, Ser. B*, **Vol. 64**, No. 624, pp212 – 219 (1998).
24. Özişik, M. N., "Basic Heat Transfer", Robert E Kriger Publishing, pp195 (1986).
25. JSME, "Flow Resistance of Pipes and Ducts", JSME, pp39 (1979).
26. Ueda, T., "Two-Phase Flow –Flow and Heat Transfer-", Yokendo Co., pp11-12, pp256-265 (1981).
27. Bergles, A. E. and Rohsenow, W. M., "The Determination of Forced–Convection Surface-Boiling Heat Transfer", *Trans. ASME, Ser. C*, **Vol. 86**, pp365 – 372 (1964).
28. Kutateladze, S. S., AEC-trans-3405, (1953).